TAO, Vol. 8, No. 1, 69-94, March 1997

A Spectral Analysis of Wave Activities and Blocking in the Northern Hemisphere Winter

Wei Min[1] and Ernest C. Kung[2]

(Manuscript received 21 November 1995, in final form 25 August 1996)

ABSTRACT

A systematic analysis of wave activities and blocking in the Northern Hemisphere winter is performed with the daily 500 mb height fields for the 1956-1991 period and the monthly sea surface temperatures (SSTs) for the 1970-1991 period. The power spectra in the wavenumber-frequency domain are partitioned into westward propagating, eastward propagating and standing variances. Regional indices are used to classify the seasonal circulation into four categories of circulation patterns according to the dominant blocking activities of the season: Pacific blocking, Atlantic blocking, double blocking, and no blocking. The distinctions among categories of blocking are characterized in the standing, westward propagating and eastward propagating variances. The distinctions are also reflected in the kinetic energy and nonlinear wave-wave interactions of the planetary-scale and the synoptic-scale waves.

A composite study of dominant circulation patterns is also presented in this study. The results show that the wave-wave interaction of the planetary-scale and the synoptic-scale waves plays a crucial role in the formation and maintenance of Pacific blocking, and that Atlantic blocking and double blocking might be forced and maintained by baroclinic processes.

(Key words: Blocking, Wave activity, Spectral analysis)

1. INTRODUCTION

In studying the low-frequency atmospheric variability, much attention has been focused on the winter blocking phenomena. Blocking circulation is important for the long-range weather forecasting for its relatively high forecasting skills and the local synoptic significance (see Shukla, 1981; Kung *et al.*, 1990 and 1992). Although most single blocking episodes have submonthly durations, monthly and even seasonal mean values of temperature and precipitation are often greatly influenced by strong, persistently recurring blockings (Rex, 1950; Namias,

[1]Data Assimilation Office, Goddard Space Flight Center, Greenbelt, Maryland 20771, U.S.A.

[2]Department of Soil and Atmospheric Sciences, University of Missouri-Columbia, Columbia, Missouri 65211, U.S.A.

1964; Quiroz, 1987). Many studies have been done concerning the mechanisms responsible for the amplification of quasi-stationary waves associated with blocking flow.

The studies of observed winter blocking have been done by analyzing the characteristics of single blocking flows in the Pacific and the Atlantic (Hartmann and Ghan, 1980; Metz, 1986; Mullen, 1987; Nakamura and Wallace, 1990). Metz (1986) analyzed the forcing of planetary flow by cyclone-scale eddy vorticity fluxes with the observation and model simulations. Mullen (1987) evaluated the effects of transient eddy heat and vorticity fluxes to the mean flow. Dole (1986 and 1989) comprehensively examined the persistent anomaly patterns in the Northern Hemisphere winter circulations. He suggested that the quasi-horizontal energy dispersion is likely to account for the development of downstream anomalies. More recently, Higgins and Schubert (1994) studied the model simulated persistent Pacific anomalies. They indicated that the role of the time-mean flow and synoptic-scale eddies in the development of the persistent Pacific anomalies is different at different stages. However, the concurrent occurrence of blocking flow in both the Pacific and the Atlantic (i.e., double blocking), which has a significant impact on the regional weather over North America and Europe, possesses somewhat different characteristics from the occurrence of single blocking (DaCamara *et al.*, 1991; Min, 1995).

Kung and Baker (1986) and Kung *et al.* (1989), in their studies of observed and simulated winter blocking episodes, showed that the development of winter blocking is associated with the nonlinear wave-wave transfer of kinetic energy from synoptic-scale disturbances to planetary waves, and the successful blocking simulation depends on adequate amplification of planetary waves. Tanaka and Kung (1988) studied the observed blocking episodes with three-dimensional normal model energetics. They demonstrated an ordinary transfer of energy from the zonal baroclinic component, via synoptic-scale component, to the barotropic component of planetary waves in association with major blocking development. Nakamura and Wallace (1990) showed evidence of the enhancement of baroclinic wave activity during the onset of blocking. Lejenäs and Madden (1992) reported that 20-40% of blocks were related to traveling wave 1, whereas the percentage was small for wave 2. The statistical study of winter blocking by Hartmann and Ghan (1980) indicated that the mechanisms sustaining blocking ridges are different in the Atlantic and the Pacific regions. By studying the monthly mean circulation patterns in the Northern Hemisphere winter during a 34-year period, DaCamara *et al.* (1991) reported that the distinction between the Pacific and Atlantic blockings appears in the stationary energy component of zonal wavenumber one. Their results also demonstrated that winter blocking activities are associated with different sea surface temperature (SST) anomaly patterns.

Since Deland (1964) introduced cross-spectral analysis into the study of large-scale propagating waves, numerous studies of large-scale propagating waves may be found in literature (e.g., Hayashi, 1977; Fraedrich and Böttger, 1978; Speth and Kirk, 1981; Speth and Madden, 1983; Hansen *et al.*, 1989). However, most of the studies are based on a relatively shorter period and are restricted to a narrow latitude belt.

The main purpose of this study is to obtain the climatological characteristics of midlatitude wave activity in the wavenumber and frequency domain, and to explore the relationship of wave activity and winter blocking circulations in the Northern Hemisphere. A systematic analy-

sis of the midlatitude wave activity and blocking circulations in the Northern Hemisphere winter is performed with the daily 500 mb height fields for the 1956-1991 period. The winter seasons are grouped into four different categories of circulation patterns on the basis of intensity and location of blocking activities during the season. The large-scale circulation patterns are examined with space-time spectra, time spectra, kinetic energy, and nonlinear transfer of kinetic energy among planetary-scale and synoptic-scale waves. Further, a composite approach of winter blocking episodes during the 36 winter seasons is attempted to examine the roles of planetary-scale and synoptic-scale waves in different stages of blocking flow.

2. DATA AND SCHEMES OF ANALYSIS

2.1 Data

Daily National Meteorological Center (NMC) octagonal grid analyses of the Northern Hemisphere 500 mb height fields are used in this study. The dataset covers 36 winter seasons from 1956 to 1991. The winter season is defined as December and the following January and February. The year of the winter season is identified by the year in which January and February occur. Daily observational analyses were used at 1500 GMT from 1956 to 1957 and at 1200 GMT for the remaining 34 years. The available data were bilinearly interpolated from the 1977-point octagonal grid to the 4° x 5° latitude-longitude spherical grid from 18°N to the pole. The missing data were interpolated linearly in time at each spherical grid point. Fourier transforms of the 500 mb height for zonal wavenumbers were then computed at the latitude circle on a daily basis. Wind components were obtained by the geostrophic approximation. The resulting time-dependent cosine and sine coefficients of height are treated as separate time series for the 36 winter seasons, starting at November 15 and lasting for 120 days. Temporal Fourier transform was utilized to determine 60 harmonic coefficients. Next, the power spectrum, the co-spectrum and the quadrature are estimated from the temporal Fourier coefficients. The spatial harmonics were cut off at wavenumber n=12, beyond which the remaining zonal variance was verified to be negligibly small. A running average over five adjacent frequencies was applied to each spectral estimate of power spectra, co- and quadrature spectra with a resulting frequency resolution of 5/120 $days^{-1}$.

Monthly SST analyses were obtained from the NMC real-time analyses (Reynolds, 1988) for the period of 1970-1991. The seasonal mean SST for the winter season was obtained as the average of monthly means of December, January and February (DJF). Cross correlation analyses with SST were based on the 22-year datasets.

2.2 Schemes of Analysis

The space-time spectral analysis is applied in this study (Pratt, 1976; Hayashi, 1977). The power spectrum of eastward propagating ($+\omega$) and westward propagating ($-\omega$) waves $E(n, \pm\omega)$ can be evaluated by the formula,

$$E(n,\pm\omega) = \frac{1}{4}[P_{\omega}(C_n) + P_{\omega}(S_n)] \pm \frac{1}{2}Q_{\omega}(C_n, S_n) \quad (1)$$

where C_n and S_n are the cosine and sine coefficients of zonal Fourier transform, n the wavenumber, and ω the frequency. Further, P_{ω} and Q_{ω} are the power spectrum and quadrature spectrum, respectively.

Hansen *et al.* (1989) compared several approaches of the partitioning techniques of the space-time spectral into standing and traveling parts. He pointed out that these techniques are qualitatively comparable. By following Hayashi's approach of partitioning of the space-time spectra into standing and traveling wave parts (see Hayashi, 1977), the standing variance $ST(n, \omega)$ and the traveling variances $TV(n, \pm\omega)$ are respectively expressed as.

$$ST(n, \omega) = [\frac{1}{4}(P_{\omega}(C_n) - P_{\omega}(S_n))^2 + K_{\omega}^2(C_n, S_n)]^{\frac{1}{2}} \quad (2)$$

$$TV(n, \pm\omega) = E(n, \pm\omega) - \frac{1}{2} ST(n, \omega) \quad (3)$$

where K_{ω} is the co-spectrum.

The procedure for identifying the blocking patterns follows that of Lejenäs and Økland (1983) and Kung *et al.* (1989, 1990, 1992, 1993):

$$I(\lambda) = Z(\lambda, 58°N) - Z(\lambda, 38°N) \quad (4)$$

where $I(\lambda)$ is the blocking index at longitude λ, Z the 500 mb geopotential height. Positive values of $I(\lambda)$ indicate the existence of anticyclone or well-defined ridge.

In the current study, we attempt to utilize the regional circulation indices to classify the winter season circulation patterns. The focus of this classification is on the characteristics of dominant circulation patterns. Two regional indices, I_{PAC} and I_{ATL}, are introduced separately for the Pacific (160°E-120°W) and Atlantic (60°W-20°E) sectors. Monthly mean indices are obtained as the monthly averages of the daily values. The regional monthly indices are thereafter normalized with respect to their means and standard deviations during the 36-year period. The seasonal indices are obtained as the average of DJF normalized I_{PAC} and I_{ATL} for the 36 years. By examining the seasonal indices, winter circulation patterns can be grouped into four categories:

(1) PAC: Dominated by Pacific blocking with positive I_{PAC} and negative I_{ATL};

(2) ATL: Dominated by Atlantic blocking with positive I_{ATL} and negative I_{PAC};

(3) DBL: Concurrent existence of blockings or sequential blockings in the Pacific and Atlantic with positive values of I_{PAC} and I_{ATL};

(4) NBL: Without the dominance of either Pacific or Atlantic blocking with negative values of I_{PAC} and I_{ATL}.

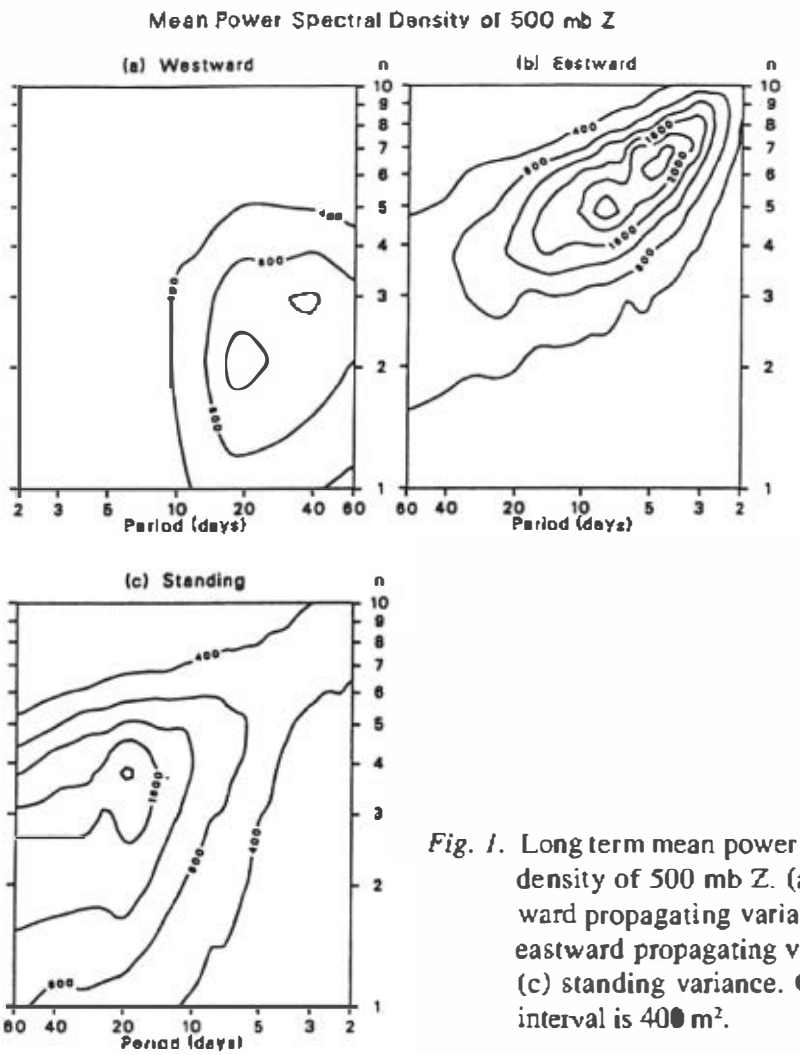

Fig. 1. Long term mean power spectral density of 500 mb Z. (a) westward propagating variance; (b) eastward propagating variance; (c) standing variance. Contour interval is 400 m^2.

The evaluation of the kinetic energy at wavenumber *n*, K(n), and the nonlinear transfer of kinetic energy from wavenumber *m* to *n*, L(n,m), follows DaCamara *et al.* (1991) and Kung *et al.* (1993), and is detailed in DaCamara (1991). A comprehensive energetic description is not possible with the restricted dataset in this study except for kinetic energy and nonlinear wave-wave interactions at 500 mb level, and the vertical flux term is not involved in computation of the nonlinear wave-wave interaction terms.

3. WAVENUMBER AND FREQUENCY SPECTRA

In this study, emphasis is placed on the midlatitude wave activities in the Northern Hemisphere. The following presentations are for the computational results averaged in the 42°-62°N latitude belt, unless otherwise specified.

The long-term mean spectral density of 500 mb Z is shown in Figure 1. The spectra are

Table 1. Power spectra of 500 mb Z for different wavenumbers and frequency bands at three latitude belts. Unit: 100 m^2.

n	18°-38°N			42°-62°N			66°-86°N		
	20-60 days	8-15 days	3-6 days	20-60 days	8-15 days	3-6 days	20-60 days	8-15 days	3-6 days
	Westward Propagating Waves								
1-3	2.47	1.14	0.54	18.97	7.47	1.19	27.40	9.99	1.36
4-9	1.48	0.61	0.07	3.88	0.84	0.16	0.64	0.41	0.26
10-14	0.03	0.02	0.03	0.05	0.07	0.13	0.00	0.00	0.01
	Eastward Propagating Waves								
1-3	2.21	0.73	0.24	9.03	3.64	2.06	10.18	6.66	3.94
4-9	2.47	3.08	2.99	7.22	9.71	10.39	1.20	1.64	2.02
10-14	0.07	0.15	0.46	0.07	0.15	0.57	0.00	0.00	0.02
	Standing Variance								
1-3	3.96	1.25	0.49	21.45	7.05	2.09	28.02	11.27	3.06
4-9	2.77	1.72	0.85	7.69	4.54	2.77	1.26	1.10	1.04
10-14	0.08	0.10	0.18	0.09	0.12	0.36	0.00	0.01	0.02

displayed in a double-logarithmic presentation of the wavenumber and frequency, as in Fraedrich and Böttger (1978) and Hansen *et al.* (1989). In order to make equal areas on these diagrams represent equal variance, the spectral densities are normalized by their wavenumbers and frequencies. The results of the 36-year mean spectral densities generally agree with those by Hansen *et al.* (1989) for a period of 16 years. The westward propagating variances show a spectral peak at the ultralong waves (n=2-3) with a period of 20-40 days (Figure 1a), and the eastward propagating variances show two spectral peaks: one near n=6-7 at roughly a 5-day period and another near n=5 at about the 10-day period. The peak of the westward propagating variances occurs at n=2-3 instead of n=1, as in Madden (1983) and Speth and Kirk (1981), because of the normalization. The standing variance (Figure 1c) shows its largest power at n=2-4 and reaches its peak at n=4 at about a 20-day period.

Table 1 gives the mean power spectra of 500 mb Z for different wavenumbers and frequency bands at three latitudinal belts of 18°-38°N, 42°-62°N and 66°-86°N. It is seen that the power spectra of the short waves n=10-14, compared with other waves, are negligibly small and the power spectra of the planetary-scale waves n=1-3 increase as the latitude increases poleward. For the planetary-scale waves, the westward propagating variances are more pronounced at the low-frequency band (T=20-60 days) in the mid and high latitudes. The synoptic-scale waves (n=4-9) show dominant eastward motion in the midlatitudes at the short period (T=3-6 days). The standing variances have the largest power for n=1-3 at the low-

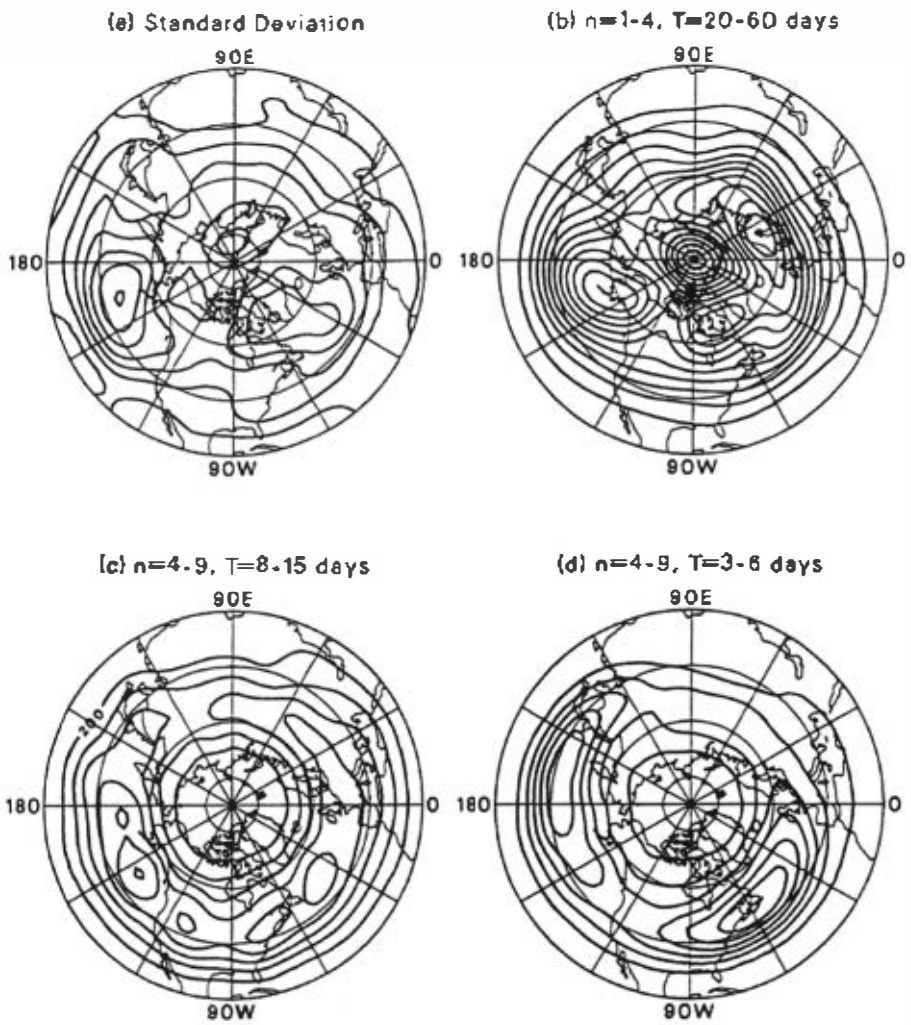

Fig. 2. Standard deviation of 500 mb Z (a) and the geographical distribution of time spectra of Z for n=1-4, T=20-60 days (b), n=4-9, T=8-20 days (c), and n=4-9, T=3-6 days (d). Contour intervals are 10 m, 500 m^2, 200 m^2, and 200 m^2, respectively.

frequency band in all latitude belts.

The standard deviation of 500 mb height field from the long-term seasonal mean field for the data period of 1956-1991 is display in Figure 2a. It shows three centers of large variability in the Northern Hemisphere circulation: the eastern North Pacific, the North Atlantic, and the arctic region of the eastern hemisphere. The locations of the three centers are in general agreement with those of Blackmon *et al.* (1976) although slight differences exist. These differences may be related to the relatively short datasets and the removal of the seasonal cycles in their studies. As Blackmon *et al.* (1986) and Metz (1986) demonstrated, these centers are also the

preferential regions of winter blockings. The center in the North Pacific is extensively located between the dateline and 150°W, indicating the importance of the Northern Pacific region in the variation of the Northern Hemisphere winter circulation. The long-term mean time spectra of 500 mb height for the low-frequency planetary-scale waves (n=1-4, T=20-60 days), the medium-range synoptic-scale waves (n=4-9, T=8-15 days) and the short-period synoptic-scale waves (n=4-9, T=3-6 days) are presented in Figures 2b-d, respectively. Three maxima of the time spectra of the planetary-scale waves are clearly seen (Figure 2b). The locations of these maxima are very close to the standard deviation maxima (Figure 2a), indicating that the variability of the winter circulation in the Northern Hemisphere is mainly attributable to the low-frequency planetary-scale waves. For the medium-range synoptic-scale waves (Figure 2c), the time spectra show maximum values in the midlatitudes over the eastern Pacific and western Atlantic, respectively, indicating the contribution of long-lived cyclones and/or anti-cyclones to the atmospheric variability. A noteworthy characteristic of the time spectra of the short-period synoptic-scale waves is the two maxima over the western Pacific and the western Atlantic along the paths of the winter storm track where the baroclinic instability is the largest. These maxima are closely associated with the winter baroclinic wave activity in the midlatitudes.

It is generally recognized that the SST anomalies exert a major forcing on the winter circulation through heat release in the ocean-atmosphere system (e.g., Namias, 1964; Shukla, 1986; Kung *et al.*, 1990). The GCM study by Mechoso *et al.* (1987) has suggested that warm equatorial Pacific SST anomalies associated with the ENSO may act to enhance high frequency, intermediate scale wave activity in the Northern Hemisphere midlatitudes. However, the low-frequency atmospheric variability is also linked to slow changes in external forcing (e.g., Horel and Wallace, 1981; DaCamara *et al.*, 1991; Kung *et al.*, 1993). Figure 3 shows the correlation of SSTs with the power spectra of 500 mb Z for the westward propagating planetary-scale waves (n=1-3) with T=20-60 days, and the eastward propagating synoptic-scale waves (n=4-9) with T=3-6 days for the period of 1970-1991. The correlation coefficient of 0.40 is at 5% significance level. It is seen that the relationships between SST forcing and the planetary-scale wave activity are quite different among wavenumbers. The westward propagating planetary-scale waves are associated not only with the equatorial SSTs but also with the midlatitude SSTs. However, the eastward propagating synoptic-scale waves show a high positive correlation with the SSTs in the western and central Pacific and negative correlations near the west coast of North America. A broad region of negative values is found in the North Atlantic sector. These may suggest that the synoptic-scale wave activity in the northern midlatitudes is associated with the SST anomalies over the midlatitude ocean.

4. DOMINANT WINTER CIRCULATION PATTERNS AND WAVE ACTIVITIES

4.1 Spectral Analysis

Table 2 presents the classification of the 36 winter seasons for 1956-1991, according to the specified categories of circulation: PAC, ATL, DBL, and NBL. The normalized values of I_{PAC} and I_{ATL} are also given. It is cautioned that the classification of seasonal circulation patterns is based on the blocking index, not on the actual occurrence of blocking episodes al-

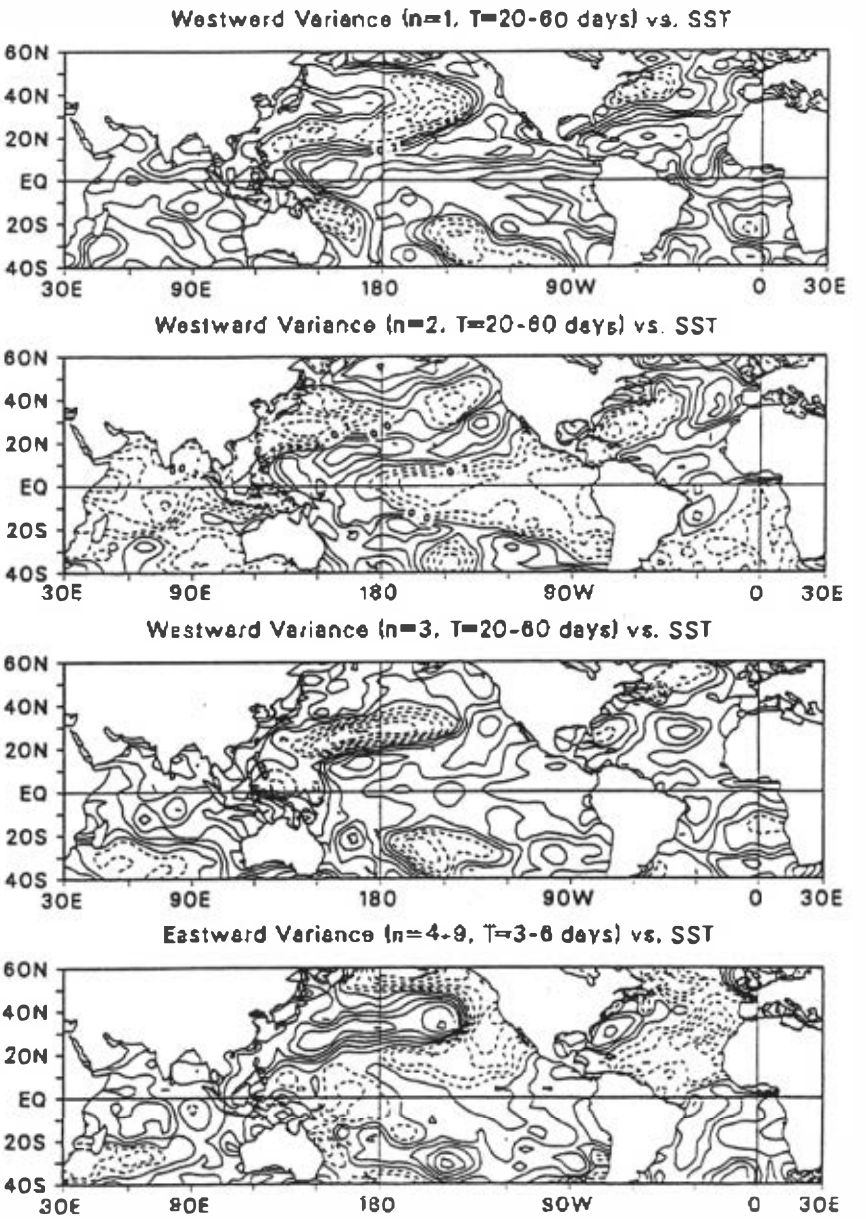

Fig. 3. Correlation patterns of SSTs with (a) westward propagating variance (n=1, T=20-60 days), (b) westward propagating variance (n=2, T=20-60 days), (c) westward propagating variance (n=3, T=20-60 days) and (d) eastward propagating variances (n=4-9, T=3-6 days). Contour interval is 0.1.

though there is a general agreement between them. The anomaly patterns for PAC, ATL and DBL clearly show the dipole structures in the respectively preferred regions of blocking for-

Table 2. Normalized blocking indices, I_{PAC} and I_{ATL}, for the 36 winter seasons.

Year	I_{PAC}	I_{ATL}	Class	Year	I_{PAC}	I_{ATL}	Class
1956	0.49	0.14	DBL	1974	0.72	-0.65	PAC
1957	0.86	-0.24	PAC	1975	-0.66	-0.49	NBL
1958	-0.51	-0.14	NBL	1976	-0.66	0.02	NBL
1959	-0.61	-0.44	NBL	1977	-0.66	-0.48	NBL
1960	-0.71	-0.04	NBL	1978	0.40	-0.39	PAC
1961	-0.21	-0.61	NBL	1979	-0.51	0.10	ATL
1962	1.01	0.44	DBL	1980	1.03	-0.15	PAC
1963	1.83	2.12	DBL	1981	0.41	-0.15	PAC
1964	-0.71	0.77	ATL	1982	0.05	-0.52	NBL
1965	0.17	2.29	DBL	1983	-0.42	0.05	NBL
1966	-0.60	-0.62	NBL	1984	0.98	-0.49	PAC
1967	-0.44	0.19	ATL	1985	-0.34	-0.35	NBL
1968	1.00	0.26	DBL	1986	0.52	-0.60	PAC
1969	-0.15	-0.05	NBL	1987	-0.60	0.39	ATL
1970	-0.35	0.22	ATL	1988	-0.51	-0.36	NBL
1971	-0.22	0.91	ATL	1989	-0.28	-0.79	NBL
1972	-0.09	0.00	NBL	1990	-0.47	-0.56	NBL
1973	-0.17	0.10	ATL	1991	0.44	0.11	DBL

mation (Figure 4). For NBL, the anomaly field shows a reversed weak dipole structure with negative anomalies in the north and positive anomalies in the south.

Madden (1983) found that the interference of stationary and propagating waves of the same longitudinal scale causes time variations in the large-scale circulation. Quiroz (1987) and Lejenas and Madden (1992) examined the relationship between blocks and large-scale westward-propagating waves. They suggested that the reinforcement of ridges by retrogressing n=1 played an important role in the occurrence of blocking. Figure 5 shows the differences of power spectral density of 500 mb height from NBL for PAC, ATL and DBL. It is noted that the major difference occurs at the low-frequency planetary-scale and the high-frequency synoptic-scale waves. For PAC, strong positive values are seen in the westward propagating variances at wavenumbers n=1-4 with a larger than 10-day period, indicating the amplification of the westward propagating planetary-scale waves during the occurrence of PAC. The eastward propagating variances show large negative values at $n \geq 5$ with a less than 15-day period, indicating the attenuation of the synoptic-scale wave activities when PAC dominates in the winter season. For the standing variance, slight increases can be seen in the low-frequency planetary-scale waves.

For ATL, the westward propagating variance only slightly increase at the low-frequency portion ($T \geq 20$ days) with maximum at n=3 and $T \geq 40$ days (Figure 5b). For the eastward propagating variance, a large positive value is seen at n=6 with a period around 5 days, indicat-

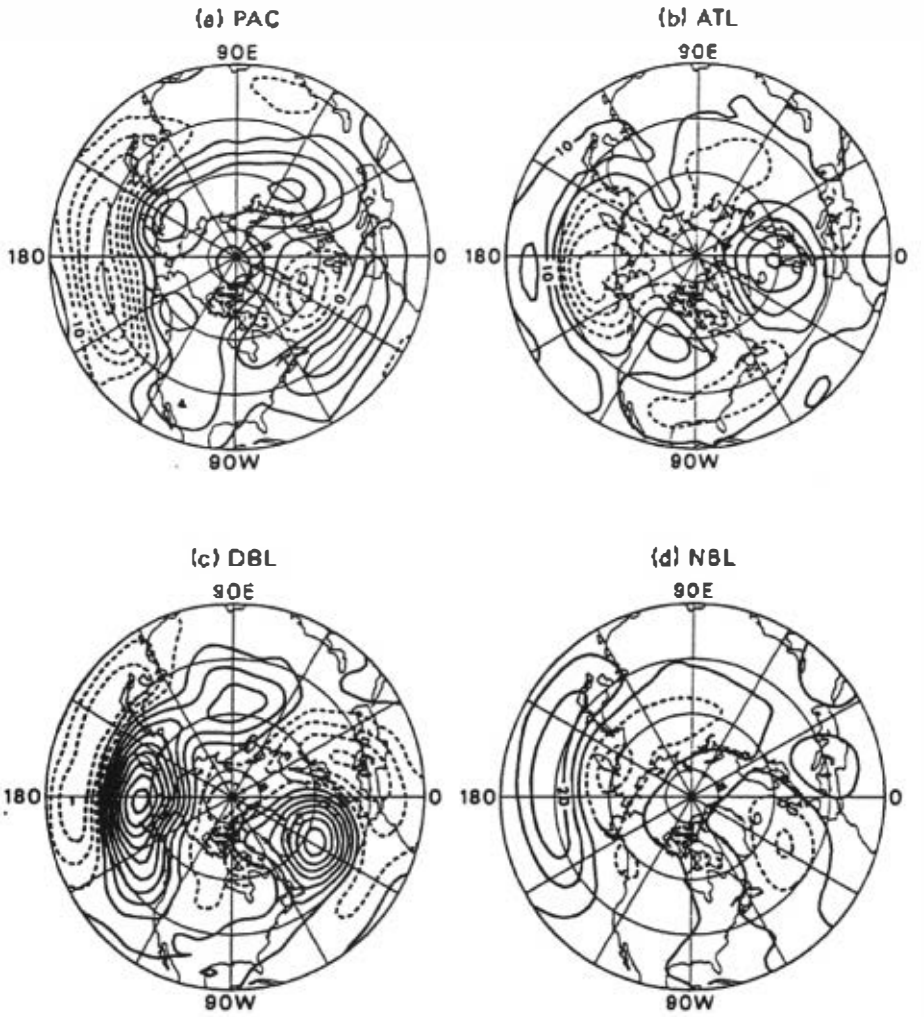

Fig. 4. Composite mean of 500 mb Z anomaly patterns for PAC, ATL, DBL and NBL. The anomalies are defined as the departure from the 36 winter season means. Contour interval is 10 m.

ing the strengthening of the synoptic-scale waves during the occurrence of ATL. Under the double blocking situation, the westward propagating variance and the standing variance are the most prominent (Figure 5c). The maximum values of the westward propagating variance are found at n=2 with around a 20-day period. The standing variance shows large positive values at n=2-4 with $T \geq 10$ days, which is consistent with the characteristics of the observed composite anomaly field. The eastward propagating variance for DBL shows generally the same features as that for PAC, with large negative values at the intermediate and short time scales for the synoptic-scale waves.

Figure 6 shows the differences of the time spectra between blocking situations (PAC,

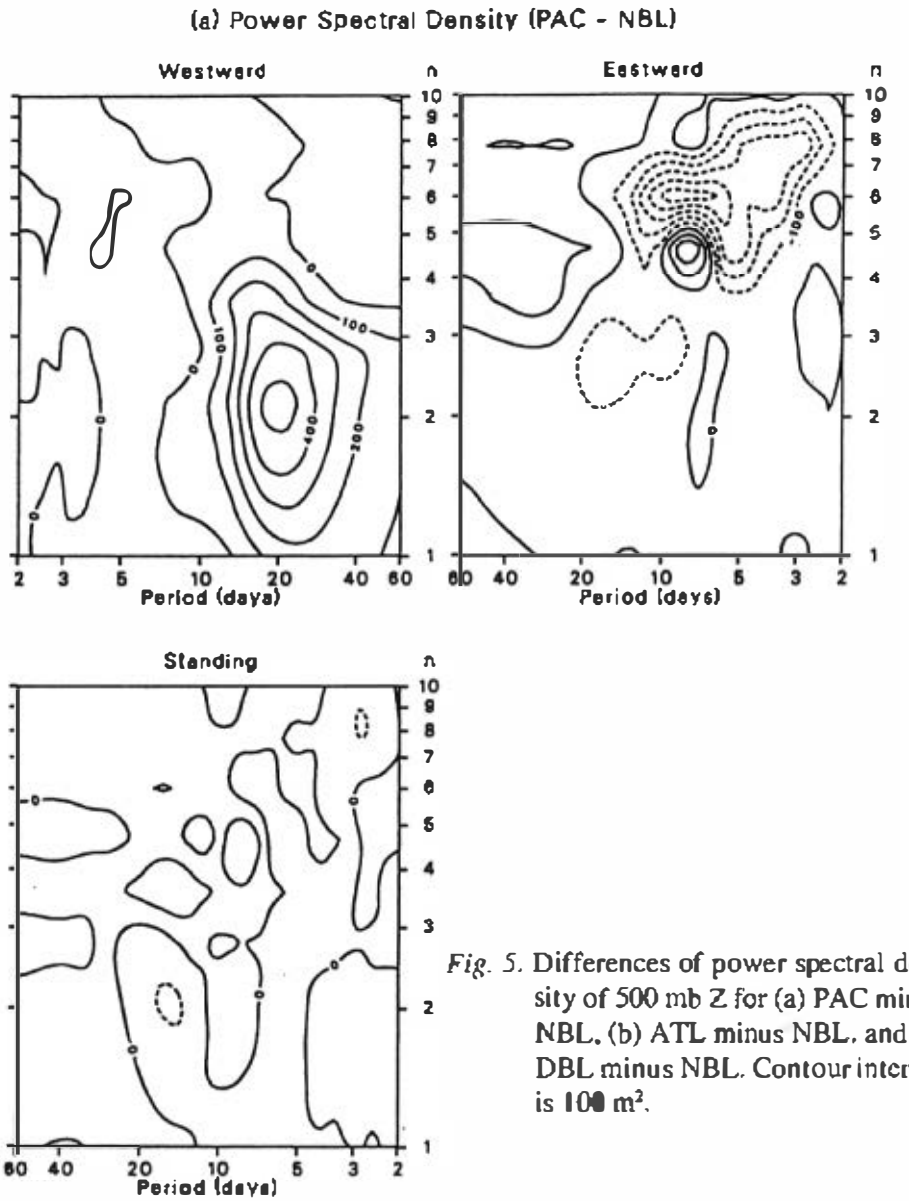

Fig. 5. Differences of power spectral density of 500 mb Z for (a) PAC minus NBL, (b) ATL minus NBL, and (c) DBL minus NBL. Contour interval is 100 m^2.

ATL and DBL) and no blocking situations (NBL) for the low-frequency planetary waves (n=1-4, T=20-60 days) and the high-frequency synoptic waves (n=4-9, T=3-6 days). For the Pacific blocking, the time spectra show strong positive values near Alaska, suggesting that Pacific blocking is closely associated with the large scale low-frequency oscillations in the winter circulation. It is also noted that large negative values are found in the two winter storm track centers (Figure 6a, right), indicating the weakening of the winter storm activities in both the Pacific and the Atlantic sectors when Pacific blocking dominates in the winter season.

In the case of ATL (Figure 6b), the time spectra of the low-frequency planetary waves in

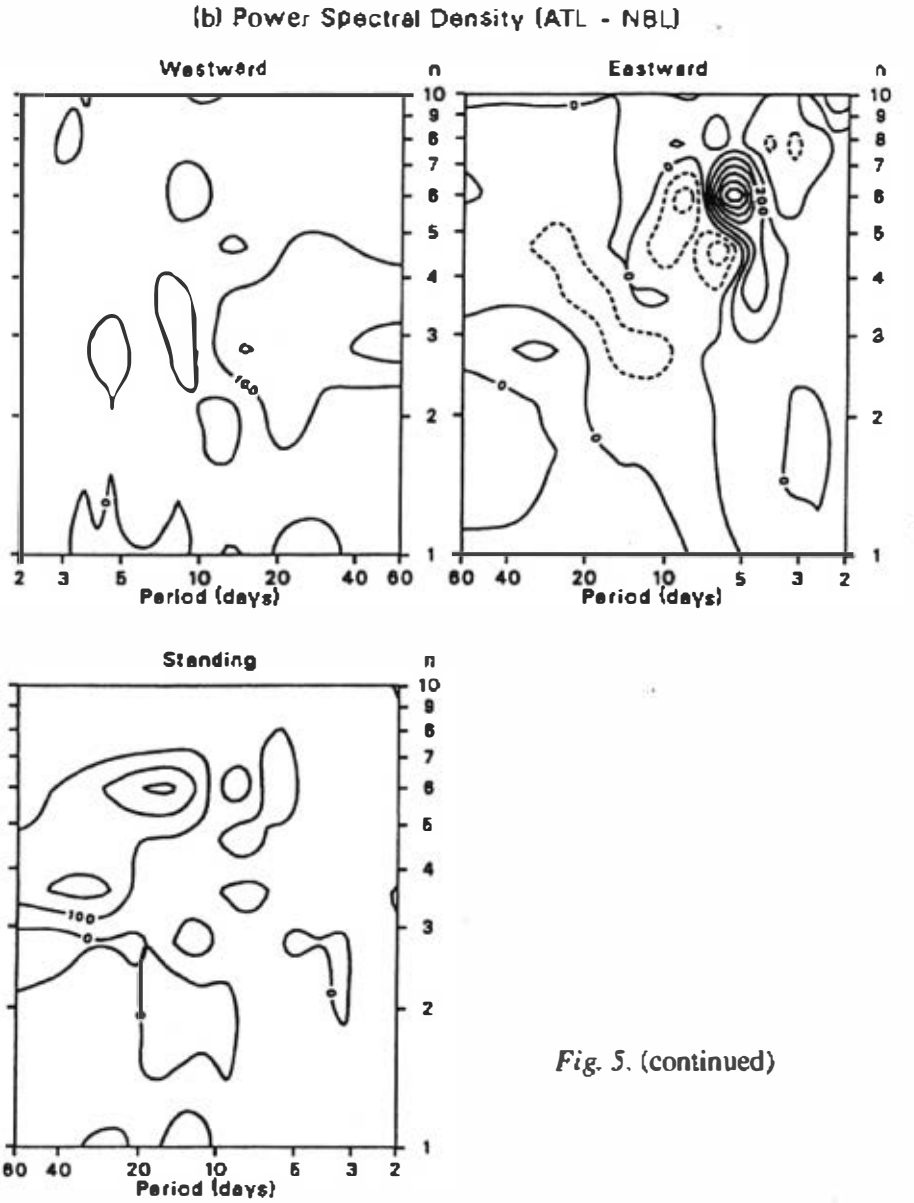

Fig. 5. (continued)

the Atlantic sector show a positive value but with smaller magnitude; whereas the time spectra of the high-frequency synoptic waves, in contrast to PAC, show large positive values in both the Pacific and the Atlantic sectors, suggesting the important roles of the transient synoptic-scale waves in the Atlantic blocking. For DBL, broad and prominent positive values are found in the northwestern hemisphere for the planetary-scale waves (Figure 6c). However, the time spectra for the high-frequency synoptic-scale waves are identical to that for PAC. This, in conjunction with the wavenumber-frequency spectra, suggest that in the occurrence of Pacific blocking (both PAC and DBL cases) the baroclinic activities in the midlatitudes are weak-

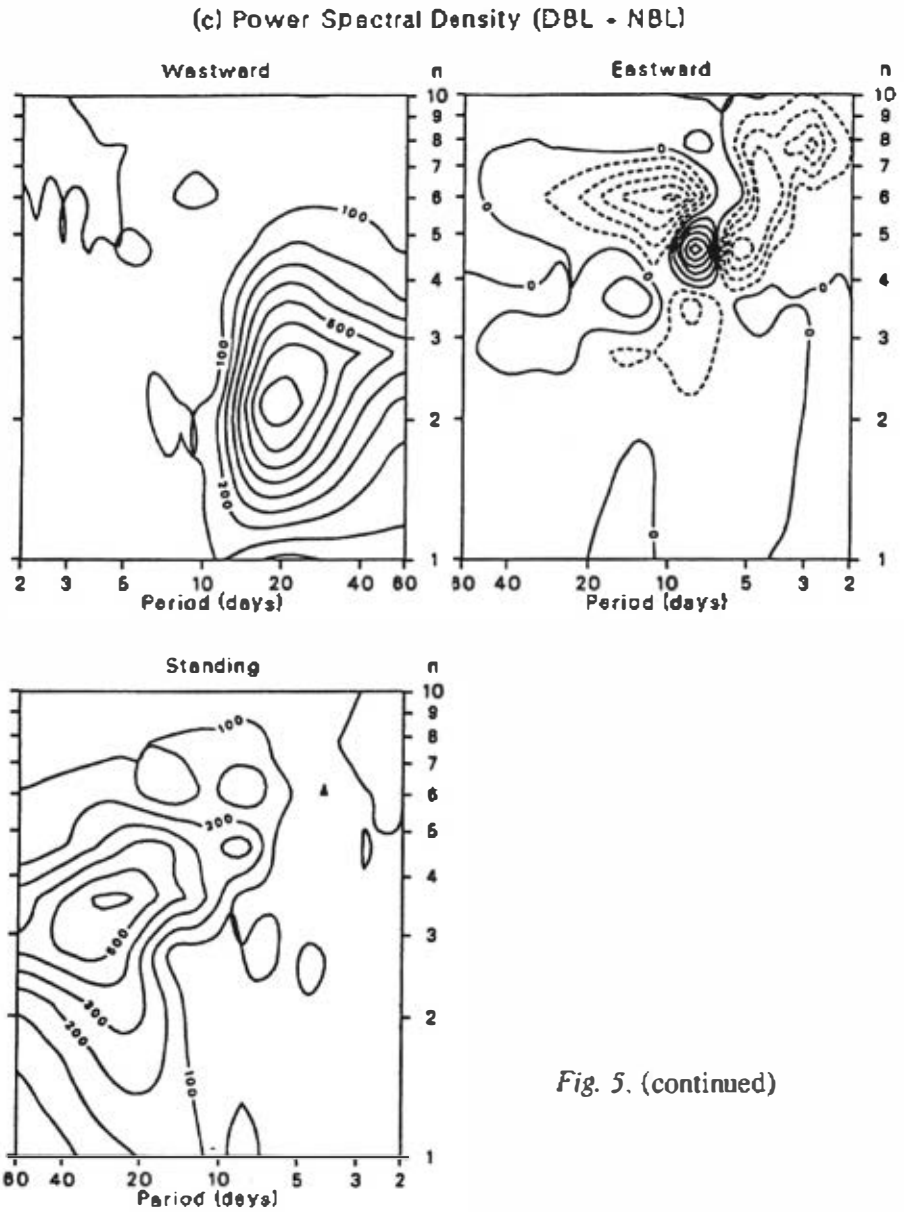

Fig. 5. (continued)

ened. The revealed enhancement of high-frequency synoptic-scale wave activity during the Atlantic blocking is consistent with Metz's (1986) study of the observed and modeled blockings. His results indicated that the forcing of planetary flow by cyclone-scale eddy vorticity fluxes was able to induce and maintain blocking highs in the Atlantic sector.

4.2 Kinetic Energy

Table 3 shows the mean kinetic energy K(n) in the 30°-62°N latitudinal belt for four cat-

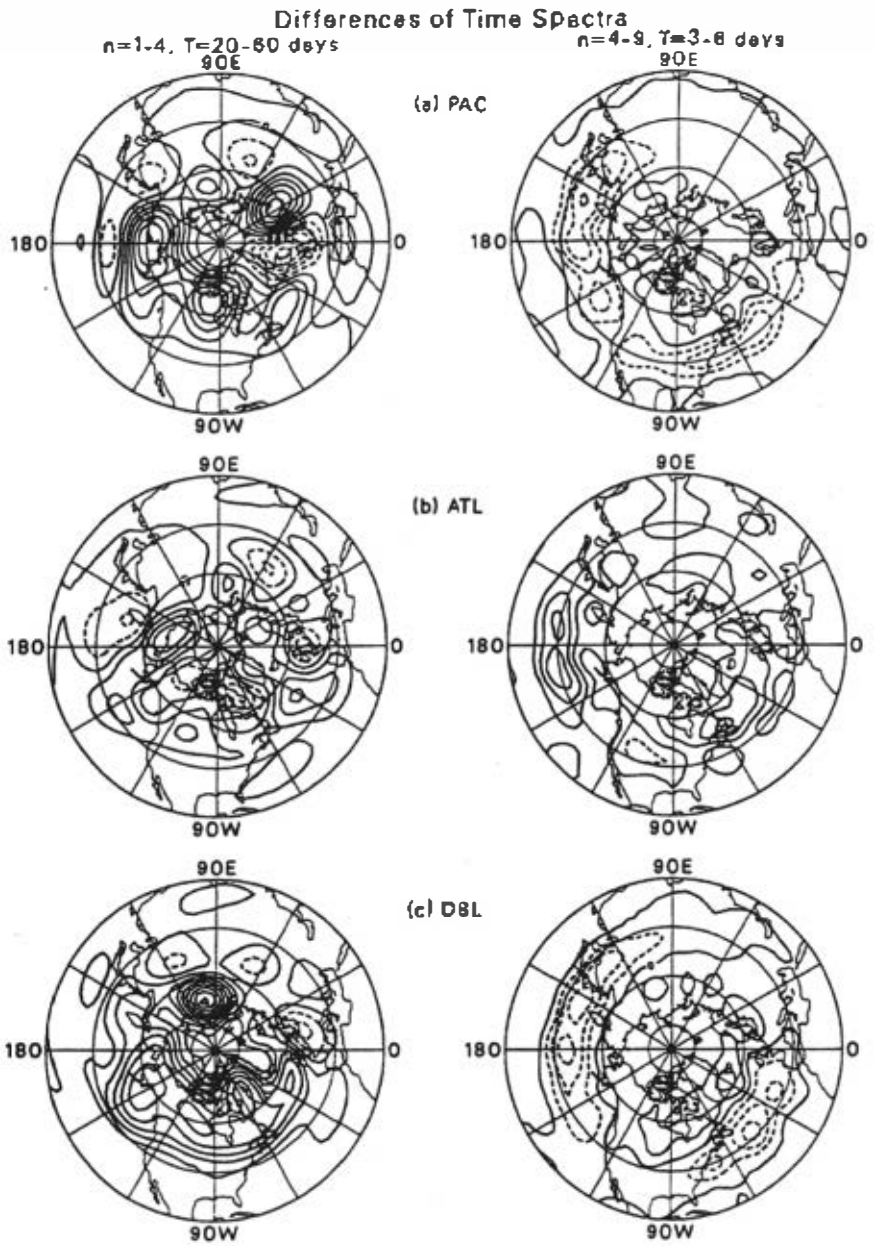

Fig. 6. Differences of power spectra of 500 mb Z for n=1-4, T=20-60 days and n=4-9, T=3-6 days for (a) PAC minus NBL, (b) ATL minus NBL, and (c) DBL minus NBL. Contour intervals are 200 and 100 m^2 for n=1-4, T=20-60 days and n=4-9, T=3-6 days, respectively.

egories of circulations. Ensemble means and standard deviations are also included. The results are consistent with the climatological study of the monthly mean circulation patterns by

Table 3. Mean kinetic energy K(n) for the four categories of blockings in the 30°-62°N latitude belt. Unit: m^2s^{-2}.

	PAC	ATL	DBL	NBL	Winter mean	Mean STD
K(1)	24.1	21.2	19.0	19.1	20.4	5.0
K(2)	20.4	20.0	21.7	20.2	20.5	3.9
K(3)	21.2	23.4	26.1	21.1	22.3	4.1
K(4-9)	58.3	66.0	65.7	60.2	61.7	6.8

DaCamara (1991) and DaCamara *et al.* (1991). Their results indicate that the difference between Pacific and Atlantic blockings is reflected in the stationary energy component of zonal wavenumber n=1. A notable difference of kinetic energy for planetary-scale and synoptic-scale waves appears among categories. The K(1) of PAC possesses the largest value among categories. For n=2 and 3, DBL shows distinctively large values. The mean K(4-9) of ATL is distinctively larger than the winter mean while K(4-9) of PAC is well below the winter season mean. This is consistent with the analyses of the power spectra and the time spectra.

Although the balance of kinetic energy depends on a number of processes, they are not all directly related to the development of blocking patterns. Kung and Baker (1986), however, pointed out that the development of a single blocking in the Pacific or Atlantic was consistently associated with an upscale kinetic energy input to n=1 through wave-wave interaction. In the situation of double blocking, the energy input is observed at n=2. In their study of monthly circulation patterns, DaCamara *et al.* (1991) indicated that the monthly values of nonlinear transfers were generally comparable with winter means without discernible monthly variation. However, the year-to-year variations of these seasonal mean values are large, as it is shown in Table 4. The mean nonlinear wave-wave transfer of kinetic energy among the planetary-scale waves for the four categories agrees with the study by DaCamara *et al.* (1991) and the major case study by Kung *et al.* (1993).

Table 4. Mean wave-wave interaction L(n,m) for the four categories of blockings in the 30°-62°N latitude belt. Unit: 10^{-5} m^2s^{-3}.

	PAC	ATL	DBL	NBL	Winter mean	Mean STD
L(1,2)	4.96	1.52	4.58	2.78	3.29	2.52
L(2,3)	1.28	0.29	1.97	-0.04	0.61	1.79
L(1,3)	-1.26	-0.91	-2.25	-1.31	-1.39	1.73
L(1,5-9)	-1.32	1.74	0.19	0.75	0.42	1.37
L(2,5-9)	1.17	-0.44	-1.09	-0.11	-0.08	1.51
L(3,5-9)	-0.43	0.32	1.64	0.03	0.25	2.05

The winter seasonal mean of the nonlinear transfer between the planetary-scale waves and the synoptic-scale waves, as listed in Table 4, shows that generally n=1 and 3 gains kinetic energy from synoptic-scale waves (n=5-9) and n=2 loses kinetic energy to n=5-9. Although these values are not significant in view of large standard deviation, the differences among categories are clearly seen. In the case of PAC, L(1,5-9) shows a distinctively large negative value and its displacement is more than one standard deviation from the ensemble mean, L(2,5-9) contrastly shows a large positive value. For ATL, the nonlinear transfer of kinetic energy to the planetary-scale waves (n=1-3) from the synoptic-scale waves (n=5-9) shows consistently positive values, indicating the important roles of the synoptic-scale waves in the formation and maintenance of the Atlantic blocking circulation. For DBL, the large negative value of L(2,5-9) indicates that, during the occurrence of double blocking, n=2 transfers kinetic energy not only to n=1 but also to the synoptic-scale waves through nonlinear wave-wave interaction. This supports the argument by Kung *et al.* (1993) that the double blocking is baroclinic in nature. The dominant n=2 should be supported by the baroclinic energy source and may become the barotropic kinetic energy source to other wavenumbers.

4.3 Blocking Episodes and Time Series Analysis

The daily values of I_{PAC} and I_{ATL} are used to determine the blocking episodes in the Pacific and Atlantic sectors. Blocking episodes are selected as those stationary anticyclonic circulations lasting for more than 10 consecutive days. The following presentations and discussions are based on the composite means of 18 Pacific blocking episodes, 15 Atlantic blocking episodes, and 16 double blocking episodes, respectively although there exist episode-to-episode variations. The onset date and the duration for each episode are listed in Table 5.

Figure 7 shows the composite mean flow patterns and anomaly fields of 500 mb height, which generally illustrate the same features as the climatological study. Austin (1980) reported that n=1 and 2 tend to interfere constructively in the Atlantic sector, and n=2 and 3 interfere in the Pacific sector. In the study of Kung *et al.* (1990), it was suggested that during the development of a Pacific blocking in January 1979, n=1 and 2 came in phase at the location of the blocking, and later the interference of n=1 and 2 in the Atlantic was identified with the development of a major Atlantic blocking. Figure 8 demonstrates the 500 mb trough-ridge diagram in the 54°- 70°N latitude band. Although the blocking indices are defined between 38°- 58°N to account for the circulation patterns, the 54°- 70°N is used in this application because it is the latitudinal band in which the ridge is maximized (Kung *et al.*, 1993). The "0" day marks the onset of blocking. It is noted that the planetary-scale waves n=1-3 interfere constructively in the longitudinal segments where blocking occurs. During the onset of Pacific blocking, traveling wave n=1 come in phase with the quasi-stationary wave n=2. For Atlantic blocking, n=1 amplifies at its normal position and reaches a peak 4-5 days after the onset of the blocking ridge. In the double blocking situation, strong amplification of n=2 is found during the onset of blocking. As Madden (1983) indicated, the interference of stationary waves and traveling waves of the same longitudinal scale cause the time variations in the large-scale circulation.

Figures 9-11 are the composite time evolutions of K(n) and L(n,m). The x-axis denotes

Table 5. Onset dates and durations for individual cases of blocking episodes.

Pacific Blocking									
Case No.	Year	Month	Day	Duration (days)	Case No.	Yea	Month	Day	Duration (days)
1	55	12	13	12	10	74	1	1	11
2	57	1	23	12	11	77	12	24	14
3	58	12	4	11	12	78	12	28	10
4	60	1	17	10	13	80	2	10	10
5	62	1	16	10	14	82	2	1	12
6	65	1	2	10	15	82	12	28	14
7	66	12	1	11	16	83	12	17	13
8	71	1	24	13	17	88	1	31	11
9	72	12	1	10	18	89	2	2	15
Atlantic Blocking									
Case No.	Year	Month	Day	Duration (days)	Cas No.	Year	Month	Day	Duration (days)
1	56	2	8	16	9	75	12	7	12
2	57	2	12	12	10	76	12	22	10
3	58	1	17	10	11	79	1	17	12
4	64	1	9	14	12	83	2	6	15
5	67	1	3	12	13	87	12	1	11
6	67	12	7	13	14	88	2	19	11
7	69	2	11	11	15	90	12	2	14
8	70	12	21	12					
Double Blocking									
Case No.	Year	Month	Day	Duration (days)	Case No.	Year	Month	Day	Duration (days)
1	57	1	9	10	9	68	2	9	10
2	59	2	7	10	10	72	2	19	10
3	61	1	17	10	11	73	1	2	10
4	62	2	19	10	12	75	1	31	10
5	62	12	22	10	13	77	12	3	10
6	63	1	10	13	14	85	1	3	12
7	63	1	26	10	15	86	2	10	13
8	64	12	17	10	16	91	1	20	10

the magnitude and the y-axis the relative day to the onset of blockings. The onset day is marked as "0" day. The differences of the K(n) and L(n,m) are clearly seen between different blocking situations. For the Pacific blocking, K(2) and L(2,3) increase and reach their peaks at day 4.

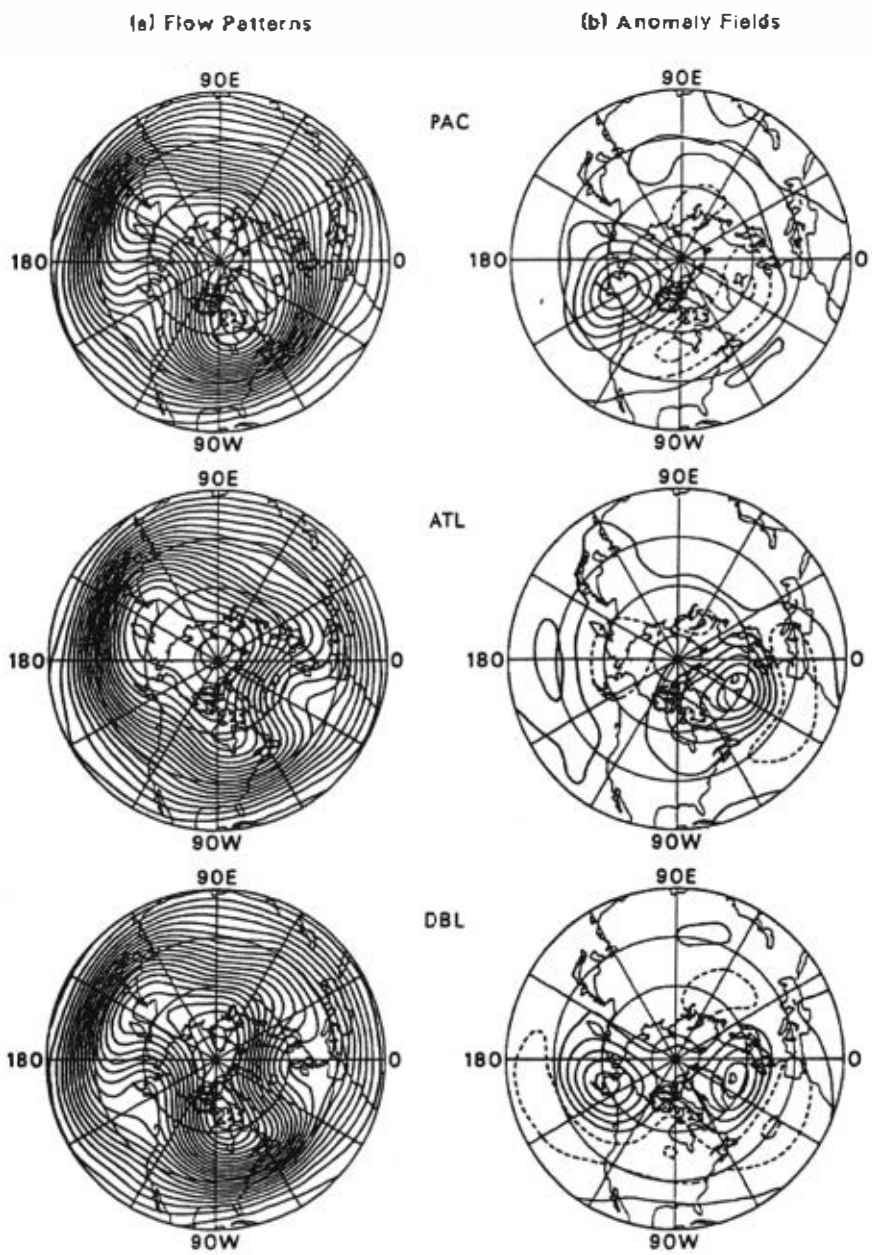

Fig. 7. The composite flow patterns and anomaly fields of 500 mb Z for Pacific blocking, Atlantic blocking and double blocking. The contour interval is 40 m. The anomalies are defined as the departures from the monthly means.

indicating that n=2 has its source at n=3 in forming the Pacific blocking. The synoptic-scale waves also contribute to the maintenance of n=2 after the onset. Subsequently, K(1) and K(3)

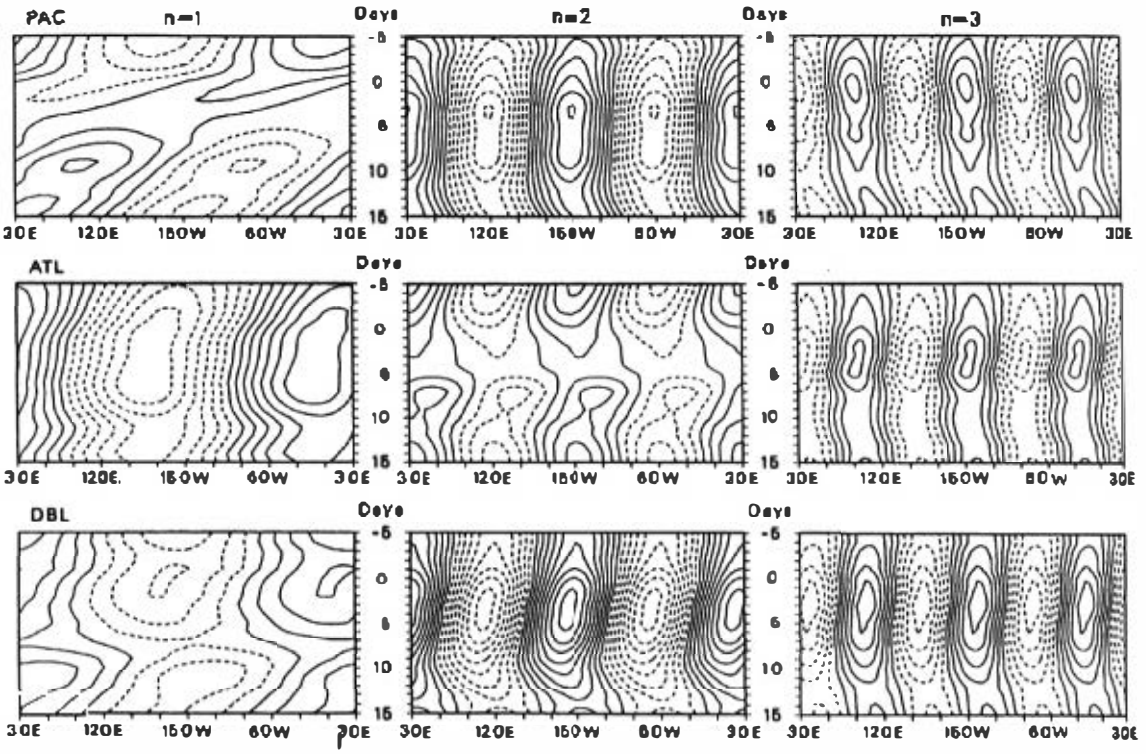

Fig. 8. The composite ridge-trough diagrams of 500 mb Z for n=1, 2 and 3 in the 54°-70°N latitude belt. The contour interval is 40 m. The "0" in the ordinate denotes the onset day of blocking episodes.

reaches their maxima about 3-5 days later than K(2). Tanaka and Kung (1988) reported that the increase in the barotropic energy of ultra-long waves through nonlinear wave-wave interaction peaks 3 days later than the increases in the baroclinic energy of synoptic-scale waves through baroclinic instability.

In the case of double blocking, K(2) and K(3) increase simultaneously and reach their peaks at day 4, whereas K(1) decreases after the onset of blocking without adequate transfer of kinetic energy from n=2 (as seen in Figure 10). It is of interest to note that L(3, 5-9) reaches its peak 1 to 2 days before the peaks of K(3), which suggests that n=3 may be maintained by the synoptic-scale wave in the double blocking case. However, the kinetic energy of planetary-scale waves (n=1-3) for the Atlantic blocking shows no evidence of significant increase except that two days before the onset K(1) reaches its maximum. This may suggest that the blocking circulation in the Atlantic, in lack of adequate amplification of planetary-scale waves, might be forced by different mechanisms. The kinetic energy of the synoptic-scale waves (n=4-9) for the Pacific blocking shows no significant changes during the 10 day period after the onset of blocking. For the Atlantic blocking, K(4-9) increases and maximizes at day 5, and fluctuates

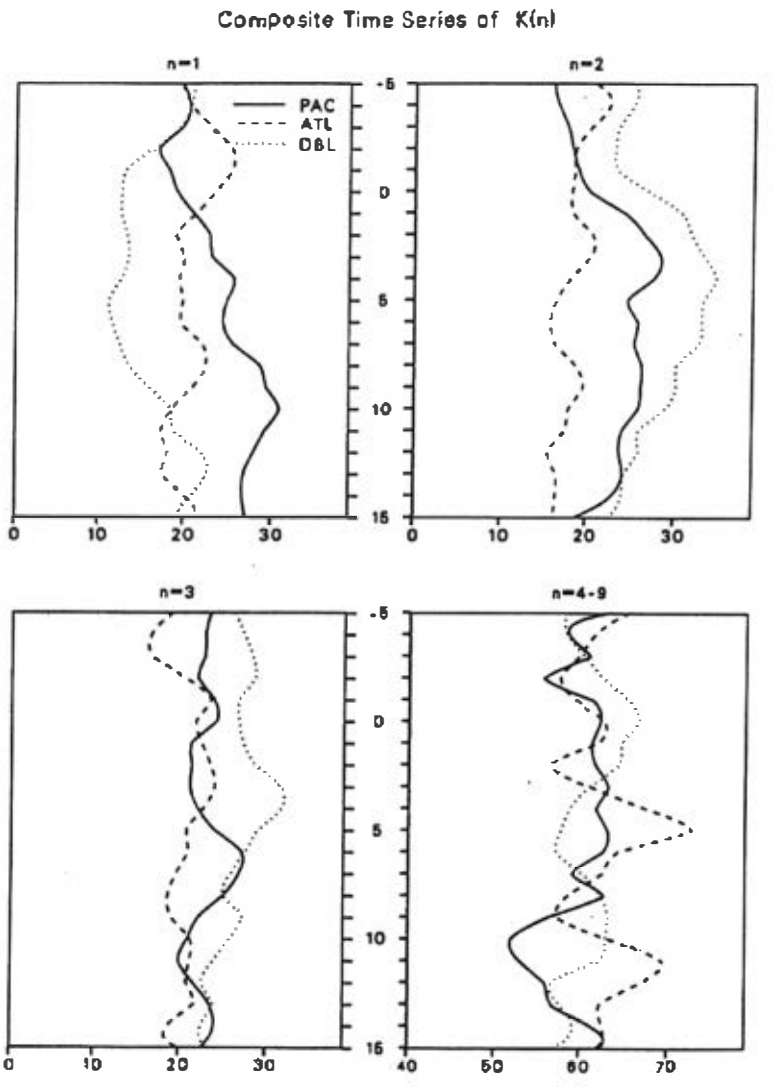

Fig. 9. The composite time series of kinetic energy K(n) in the 30°-62°N latitude belt for PAC, ATL and DBL episodes. Unit: m^2s^{-2}. The abscissa denotes the magnitude and the ordinate relative days to the onset of blockings.

in a period of about 5-6 days. During the life cycle of double blocking, the K(4-9) reaches its peak at the onset day and fluctuates in a period of about 8-10 days.

The time series of L(1,2), L(1,3) and L(2,3) in Figure 10 also show large differences between different blocking circulations. For the Pacific blocking, L(1,2) and L(2,3) increase during the course of blocking flow. A strong increase of L(1,2) after the onset is well illustrated for the Pacific blocking, indicating that n=1 carries over a large amount of kinetic energy from n=2 after the blocking is fully developed. For the Atlantic blocking and double

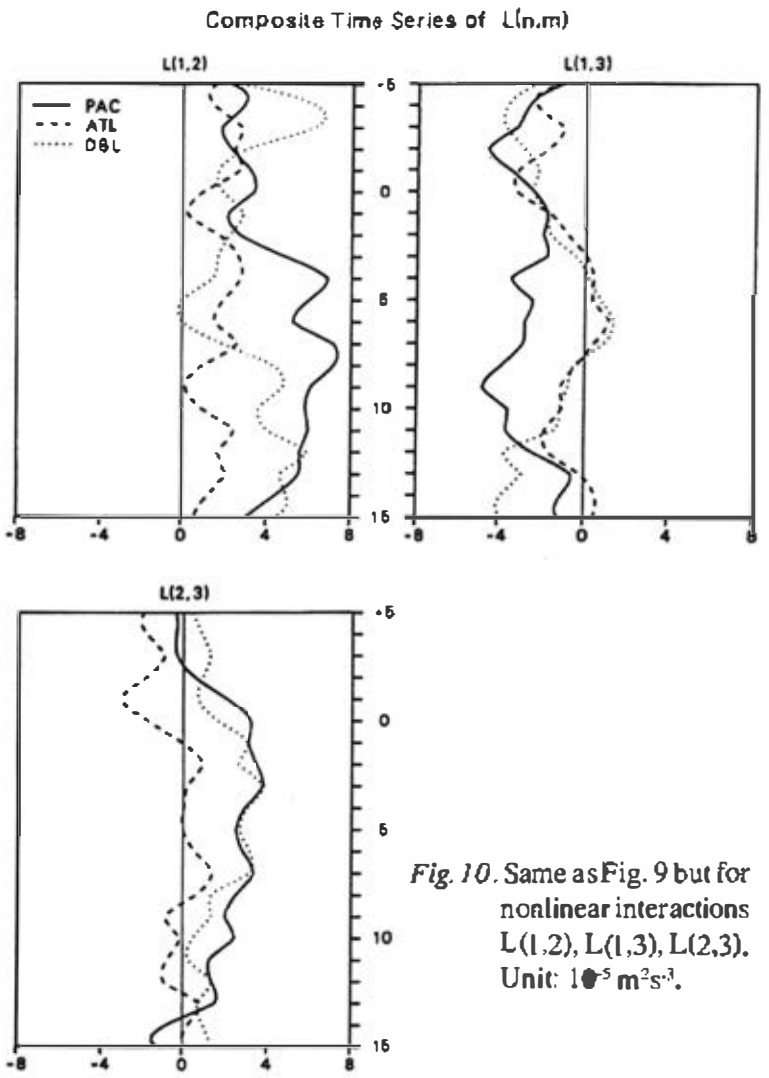

Fig. 10. Same as Fig. 9 but for nonlinear interactions L(1,2), L(1,3), L(2,3). Unit: 10^{-5} m^2s^{-3}.

blocking, L(1,3), distinguished from Pacific blocking, increases after the onset of blocking and reaches its maximum at day 5. Although L(1,3) has a small positive value at its peak, the net effect on the kinetic energy budget could be tremendous since n=3 normally receives a large amount energy from n=1 (see Table 4). It seems likely that the forcing of the planetary-scale waves by the synoptic-scale waves through nonlinear wave-wave interaction is an important factor in the life cycle of blocking, particularly for the Pacific blockings.

5. CONCLUDING REMARKS

The characteristics of wave activities in the Northern Hemisphere winter for 1956-1991 are examined using the space-time spectral analysis, and summarized in the wavenumber and

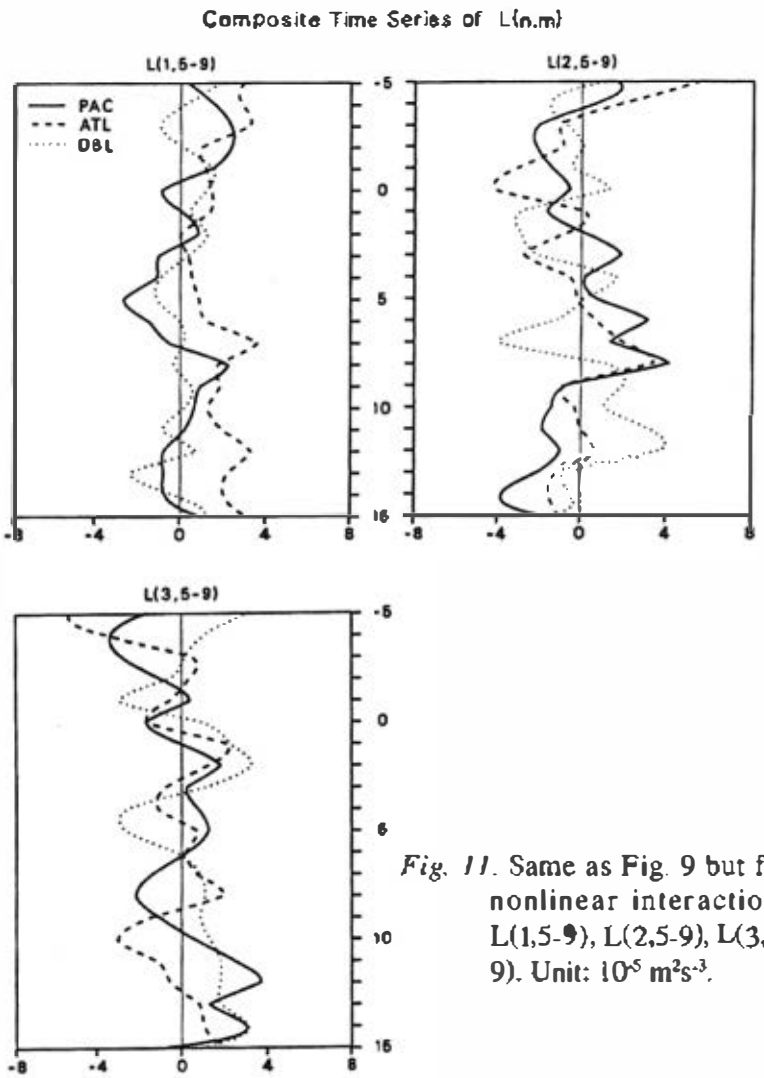

Fig. 11. Same as Fig. 9 but for nonlinear interactions L(1,5-9), L(2,5-9), L(3,5-9). Unit: 10^{-5} m^2s^{-3}.

frequency domain. The results are in reasonable agreements with the results of previously available studies with shorter period datasets (e.g., Fraedrich and Böttger, 1978; Speth and Madden, 1983; Hansen *et al.*, 1989). As revealed by the spatial distributions of time spectra, the variability of the winter circulation in the Northern Hemisphere winter is attributed to the low frequency planetary-scale waves.

The most prominent phenomenon in the winter circulation is the quasi-stationary anticyclonic ridges or blockings in the Pacific and the Atlantic. When they occur, they exert dominant influences on the local weather. Classification of the seasonal circulation in the Northern Hemisphere winter on the basis of blocking activities, as used in this study, seems to adequately identify four categories of winter circulation patterns: PAC (Pacific blocking), ATL

(Atlantic blocking), DBL (double blocking), and NBL (no blocking). Characteristics among these categories are distinguished in terms of power spectra in the wavenumber and frequency domain, kinetic energy, and nonlinear energy transfer.

The differences of the power spectra among PAC, ATL and DBL are clearly seen in the standing variance and traveling variances. It is shown in this study that Pacific blocking is associated with the strengthening of the low frequency planetary-scale waves and the Atlantic blocking is associated with the enhancement of the high frequency synoptic-scale waves. For the double blocking, standing variance shows peaks at n=2-4 with a larger than 10 day period. Different circulation patterns may involve different physical mechanisms. For the Pacific blocking, the barotropic energy transfer from n=2 to n=1 plays an important role in forming and maintaining the blocking circulation; whereas for the Atlantic blocking the source of kinetic energy to sustain the blocking circulation is the baroclinic conversion from potential energy to kinetic energy. Time series analysis indicates that synoptic-scale waves are important in the development and maintenance of Atlantic and double blocking, and that planetary-scale waves play a crucial role in the Pacific blocking.

Although it would be difficult to draw definite conclusions from this study because of the limitations of the datasets, it is demonstrated that nonlinear transfer of kinetic energy plays an important role in the formation and maintenance of dominant circulation patterns associated with winter blocking.

Acknowledgments The authors gratefully acknowledge the technical assistance of Dr. J.G. Chern, Ms. T. L. Henke and Ms. D. A. Haar. We are grateful to the two anonymous reviewers for their extensive reviews of this paper. This work was carried out as part of the first author's doctoral research under the second author's supervision in the University of Missouri-Columbia. Support for this research was provided by the National Biological Service under Cooperative Agreement USDI #1445-CA09-95-0069 #02.

REFERENCES

Austin, J.G., 1980: The blocking of middle latitude westerly winds by planetary waves. *Quart. J. Roy. Meteor. Soc.*, **106**, 327-350.

Blackmon, M.L., 1976: A climatological spectral study of the 500 mb geopotential height of the Northern Hemisphere. *J. Atmos. Sci.*, **33**, 1607-1623.

Blackmon, M.L., S.L. Mullen and G.T. Bates, 1986: The climatology of blocking events in a perpetual January simulation of a spectral general circulation model. *J. Atmos. Sci.*, **43**, 1379-1405.

DaCamara, C.C., 1991: Planetary wave activities and energetics in the Northern Hemisphere winter circulation. Ph.D. Thesis, University of Missouri-Columbia, 105pp.

DaCamara, C.C., E.C. Kung, W.E. Baker, B.-C. Lee and J.A.M. Cortel-Real. 1991: Long-term analysis of planetary wave activities and blocking circulation in the Northern Hemisphere winter. *Beitr. Phys. Atmos.*, **64**, 285-298.

Deland, R.J., 1964: Traveling planetary waves. *Tellus*, **16**, 271-273.

Dole, M. D., 1986: Persistent anomalies of the extratropical northern hemisphere wintertime

circulation: Structure. *Mon. Wea. Rev.*, **114**, 178-207.

Dole, M. D., 1989: Life cycles of persistent anomalies. Part I: Evolution of 500 mb height fields. *Mon. Wea. Rev.*, **117**, 177-211.

Fraedrich, K. and H. Böttger, 1978: A wavenumber-frequency analysis of the 500 mb geopotential at 50°N. *J. Atmos. Sci.*, **35**, 745-750.

Hansen, A.R., A. Sutera and D.E. Venne, 1989: An examination of midlatitude power spectra: evidence for standing variance and the signature of El Niño. *Tellus*, **41A**, 371-384.

Hartmann, D.L. and S.J. Ghan, 1980: A statistical study of the dynamics of blocking. *Mon. Wea. Rev.*, **108**, 1144-1159.

Hayashi, Y., 1977: On the coherence between progressive and retrogressive waves and a partition of space-time power spectra into standing and traveling parts. *J. Atmos. Sci.*, **36**, 1017-1029.

Higgins, W.R. and S. D. Schubert, 1994: Simulated life cycles of persistent anticyclonic anomalies over the North Pacific : role of synoptic-scale eddies. *J. Atmos. Sci.*, **51**, 3238-3260.

Horel, J.D. and J.M. Wallace, 1981: Planetary-scale atmospheric phenomena associated with the Southern Oscillation. *Mon. Wea. Rev.*, **109**, 813-829.

Kung, E.C. and W.E. Baker, 1986: Spectral energetics of the observed and simulated Northern Hemisphere general circulation during blocking periods. *J. Atmos. Sci.*, **43**, 2792-2812.

Kung, E.C., H.L. Tanaka and W.E.Baker, 1989: Energetic examination of winter blocking simulations in the Northern Hemisphere. *Mon. Wea. Rev.*, **117**, 2019-2040.

Kung, E.C., C.C. DaCamara, W.E. Baker, J. Susskind and C.K. Park, 1990: Simulations of winter blocking episodes using observed sea surface temperatures. *Quart. J. Roy. Meteor. Soc.*, **116**, 1053-1070.

Kung, E.C., W. Min, J. Susskind and C.K. Park, 1992: An analysis of simulated summer blocking episodes. *Quart. J. Roy. Meteor. Soc.*, **118**, 351-363.

Kung, E.C., J. Susskind and C.C. DaCamara, 1993: Prominent Northern Hemisphere winter blocking episodes and associated anomaly fields of sea surface temperatures. *TAO.*, **4**, 273-291.

Lejenäs, H. and H. Økland, 1983: Characteristics of Northern Hemisphere blocking as determined from a long time series of observational data. *Tellus*, **35A**, 350-362.

Lejenäs, H. and R.A. Madden, 1992: Traveling planetary-scale waves and blocking. *Mon. Wea. Rev.*, **120**, 2821-2830.

Madden, R.A., 1983: The effects of the interference of traveling and stationary waves on the variations of the large-scale circulation. *J. Atmos. Sci.*, **40**, 1110-1125.

Mechoso, C.R., A.Kitoh, S. Morrthi and A. Arakawa, 1987: Numerical simulations of the atmospheric response to a sea surface temperature anomaly over the equatorial eastern Pacific ocean. *Mon. Wea. Rev.*, **115**, 2936-2956.

Metz, W., 1986: Transient cyclone-scale vorticity forcing of blocking high. *J. Atmos. Sci.*, **43**, 1467-1483.

Min, W., 1995: Climatology of wave activities and blocking in the Northern Hemisphere winter. Ph.D. Thesis, University of Missouri-Columbia, 87pp.

Mullen, S.L., 1987: Transient eddy forcing of blocking high. *J. Atmos. Sci.*, **44**, 3-22.

Nakamura, H. and J.M. Wallace, 1990: Observed changes in baroclinic wave activity during the life cycles of low-frequency circulation anomalies. *J. Atmos. Sci.*, 47, 1100-1116.

Namias, J., 1964: Seasonal persistence and recurrence of European blocking during 1958-1960. *Tellus.*, **16**, 394-407.

Pratt, R.W., 1976: The interpretation of space-time spectral quantities. *J. Atmos. Sci.*, **33**, 1060-1066.

Quiroz, R.S., 1987: Traveling waves and regional transitions in blocking activity in the Northern Hemisphere. *Mon. Wea. Rev.*, **112**, 1894-1912.

Renolds, R.W., 1988: A real-time global sea surface temperature analysis. *J. Climate* , **4**, 457-467.

Rex, D.F., 1950: Blocking action in the middle troposphere and its effect upon regional climate, II: The climatology of blocking. *Tellus.*, **2**, 275-301.

Shukla, J., 1986: SST anomalies and blocking. In: R. Benzi, B. Saltzman and A.C. Wiin-Nelsen (Eds.), Anomalous atmospheric flows and blocking , Academic, 443-452.

Speth, P. and E. Kirk, 1981: A one-year study of power spectra in wavenumber-frequency domain. *Beitr. Phys. Atmos.*, **54** , 186-206.

Speth, P. and R.A. Madden, 1983: Space-time spectral analyses of Northern Hemisphere geopotential heights. *J. Atmos. Sci.*, **40**, 1086-1100.

Tanaka, H. and E.C. Kung, 1988: Normal mode energetics of the general circulation during the FGGE year. *J. Atmos. Sci.*, **45**, 3723-3736.